Intermediate Levels of Smad2 and Smad3, and Insights into TGF-β Signaling Thresholds

A Senior Honors Thesis

Presented in partial fulfillment of the requirements for graduation
with distinction in Biology in the undergraduate colleges
of The Ohio State University

by

Andrew Chow
The Ohio State University
August 2005

Project Adviser: Doctor Michael Weinstein, Department of Molecular Genetics

Thesis Committee:

Dr. Michael Weinstein
Dr. Russell Hill
Dr. Terry Gustafson

Abstract

The Smads are intracellular mediators of the signaling cascade initiated by the Transforming Growth Factor-Beta (TGF-β) superfamily of ligands. Notable ligands include TGF-β, bone morphogenic proteins (BMPs), nodal, and activins. These ligands affect a broad range of processes that including development, differentiation, homeostasis, and apoptosis. One mechanism of ligand signal regulation involves dose-dependent nature of Smad transcriptional regulation. Two distinct, although parallel, Smad pathways exist. Smads 1, 5, and 8 mediate BMP signals while Smad2 and Smad3 mediate TGF-β, activin, and nodal signals. Studies of Smad2 and Smad3 via knockout technologies reveal Smad3 functions in bone development and immune system function while Smad2 is required for gastrulation and proper development of anterior and midline structures. Combinational studies using traditional *Smad2* and *Smad3* knockout alleles uncovered a synergistic effect of Smad2 and Smad3 on liver development. Using a hypomorphic allele of *Smad2*, my studies of this interaction suggest that all abnormalities arising from insufficiencies of Smad2 and Smad3 mediation have been described, and that the abnormalities observed represent a continuum of abnormalities related to the amount of TGF-β-like signaling mediated by Smad2 and Smad3.

Table of Contents

Introduction:

The ubiquitous Transforming Growth Factor-Beta (TGF-β) superfamily of ligands controls a myriad of processes that include cell differentiation, development, angiogenesis, immune system response, apoptosis, and homeostasis. The most notable ligands of this superfamily are TGF-β, bone morphogenic proteins (BMPs), nodal, and activins [1],(reviewed in [2, 3]). TGF-β ligands initiate the cell signaling pathway by binding to their respective transmembrane Type II receptor, which activates the serine/threonine kinase domain on the receptor. This activated Type II receptor recruits a complimentary transmembrane Type I receptor and phosphorylates the glycine/serine rich domain of the Type I receptor to activate the Type I receptor's own serine/threonine kinase. The Type I serine/threonine kinase recognizes and phosphorylates a Serine Serine X Serine (SSXS) motif on the Mad homology 2 (MH2) domain of its respective receptor-activated Smad (R-Smads) (reviewed in [2, 3]). These R-Smads then form heteromeric complexes with the co-Smad (Smad4) *en route* to the nucleus where the complex will bind either with transcriptional coactivators such as p300 and induce transcription, or with transcriptional corepressors such as TGIF and repress transcription (Fig. 1).

The Smad family of intracellular mediators is divided into three categories: R-Smads, co-Smad, and inhibitory Smads (I-Smads). The hallmark of the Smad proteins is the highly conserved N-terminal Mad homology 1 (MH1) and C-terminal MH2 domains, between which lies a more variable linker region [4] (Fig. 2). The I-Smads—Smads 6 and 7—are the only Smads to lack the MH1 domain, but they possess intact SSXS motifs in their MH2 domains that allow one of their inhibitory mechanisms to operate by competitively inhibiting phosphorylation of R-Smads (reviewed in [2, 3]). The bulk of research has been focused on R-Smads and Smad4, as their signaling directly leads to transcriptional responses. R-Smads are made up of two

subfamilies. Smads 1, 5, and 8 mediate BMP ligand signals while Smads 2 and 3 mediate signals from TGF-β, nodal, and activin. R-Smad phosphorylation is dependent on binding to a specific combination of Type I and Type II receptor complexes (reviewed in [2, 3]). Unlike the specificity of the receptor complexes, Smad4 binds to all activated R-Smads to form heteromeric complexes that translocate to the nucleus to regulate transcription.

Interest in Smads has grown greatly following several reports implicating various Smads in tumorigenesis. In fact, abnormalities in all Smads of the TGF-β/activin/nodal pathway have been reported in various tumors. For instance, *Smad4* is mutated in 50% of all pancreatic tumors [4, 5]. *Smad2* expression is significantly reduced in head and neck carcinomas, while the gene itself is mutated in some lung and colorectal cancers (reviewed in [6])[7]. Finally, the loss of Smad3 is suspected of increasing susceptibility to human gastric cancer [8], while a study using the mouse model demonstrated that all *Smad3* null mice develop metastatic colorectal cancer [9].

Knowing that a gene is abnormal in a tumor provides little information about the natural function of the gene though. Understanding the natural function of the gene is important since such knowledge might assist the development of new therapies that will restore the normal function of mutated genes. The most common approaches to ascertaining the natural function of a gene are through experiments in which the gene is manipulated to either overexpress or underexpress its encoded protein. Most underexpression experiments take the form of gene knockouts to form null or hypomorphic alleles. A mouse model is ideal for underexpression experiments in several respects including short maturity time, large litter sizes (eight to fifteen), similarity between human and mouse genomes, and the relative ease and accuracy with which knockouts can be performed and studied. The nine distinct targeted disruptions of *Smad2* created since 1998 are a testament to how routine mice gene knockouts have become [10-18].

These knockouts have unveiled the importance of Smad2 during gastrulation, anterior/posterior axis determination, craniofacial development, and liver development. *Smad2* null mice fail to gastrulate, resulting in embryonic lethality around embryonic day 8.5 (E8.5). About five percent of heterozygotes are abnormal, implying that the level of TGF-β signaling in heterozygotes is hovering barely above the threshold required for successful embryogenesis [10, 11]. Although highly homologous to *Smad2* and a signal transducer for the same set of ligands, *Smad3* does not appear to be vital for embryogenesis, as *Smad3* null pups are viable. Knockouts have uncovered the roles of *Smad3* in immune system function, especially in the mucosal membranes, skeletal formation, and growth of ovarian follicles [9, 19, 20].

Because *Smad3* null mice do not exhibit embryonic lethality, the primary function of Smad3 was easily discerned for the entire lifespan of the mice. However, the embryonic lethality of *Smad2* leaves a gap of unknown function following the lethality by E8.5. One of the initial approaches to fill in the void involved the combination of *Smad2* with *Smad3* mutations. Although Smad2 and Smad3 have distinct functions [20], they are both intracellular signal transducers for TGF-β/activin/nodal ligands. Because *Smad2* heterozygotes are already hovering around the minimum threshold of TGF-β signaling required for embryogenesis, any interaction between Smad2 and Smad3 should lower the level of TGF-β signaling below that threshold and result in abnormalities, uncovering insights into *Smad2* function after E8.5. The expected combination at which lethality might occur is $Smad2^{+/-};Smad3^{-/-}$ because individually, $Smad2^{+/-}$ mice and $Smad3^{-/-}$ mice are both viable. However, a synergistic interaction between these two mediators was discovered when dissections revealed that $Smad2^{+/-};Smad3^{+/-}$ embryos do not survive past E16.5. These embryos exhibited variably penetrant phenotypes including cardiac dysplasia, axial patterning defects, craniofacial abnormalities, and hepatic dysplasia. This

experiment demonstrated that Smad2 and Smad3 cooperate during liver development, a function that was not discernable with individually *Smad2*-deficient or *Smad3*-deficient embryos [21, 22].

An alternative to combining mutations is to create conditional knockouts. Courtesy of advances in knockout technology, investigators can now regulate knockouts spatiotemporally. Many conditional knockouts utilize the Cre-loxP system. Cre is a bacteriophage recombinase with many functions, one function of which recognizes specific sequences of DNA called loxP sites, excises the genetic material between two successive loxP, and ligates the chromosome back together [23], (reviewed in [24]). A conditional *Smad2* allele was created using this Cre-loxP system to study the role of Smad2 further in development [12]. A targeting construct was created with a loxP site inserted into intron 8 and a PGK*neo* cassette flanked by loxP sites inserted into intron 10 (Fig. 3). Following electroporation of the targeting construct into ES cells and double selection for *neomycin* resistance in addition to lack of the gene for thymidine kinase, homologous recombination was screened for in DNA isolated from surviving cells by using a 5' external probe. Southern blot analysis confirmed the creation of the conditional *Smad2* allele, called $Smad2^{3loxP}$. After injection into a blastocyst and confirmation of transmission through the germline by PCR analysis, the *Smad2* allele was crossed with a mouse carrying a *Cre* transgene that would be expressed in all embryonic tissues to generate recombined alleles (Fig. 4). Genetic tests revealed that the resulting $Smad2^{\Delta E9,10}$ allele behaved similarly to the $Smad2^{-}$ allele created by Nomura *et al*. and Weinstein *et al*. in 1998 [10, 11], and that the $Smad2^{flox}$ allele was indistinguishable from the wild-type allele, thus confirming the creation of a conditional null allele [12].

In addition to allowing spatiotemporal control of the knockout, an unexpected benefit of the $Smad2^{3loxP}$ conditional allele was its hypomorphic behavior. Although it was viable and

fertile in the homozygous state, 100% of *Smad2*$^{3loxP/-}$ embryos exhibited embryonic lethality [12]. In contrast, only five percent of Smad2$^{+/-}$ embryos perished during embryogenesis [11]. This hypomorphism was attributed to the presence of the *neo* cassette. Many studies have demonstrated and taken advantage of the cryptic splice acceptor and donor sites within the *neo* cassette that cause part of the *neo* sequence to be incorporated into mRNA during transcription [12, 25, 26]. The location of the *neo* cassette in the *Smad2*^{3loxP} allele predicts a truncated, non-functional protein translation when cryptic splicing occurs and *neo* is included in the mRNA transcript, as an in-frame stop codon within the neo cassette terminates translation before the SSXS motif required for *Smad2* phosphorylation. Other genetic experiments confirmed that the *neo* cassette was the culprit of the hypomorphism and that the alleles were segregating independently [12].

Results:

Although genetic experiments confirmed the hypomorphism of the *Smad2*^{3loxP} allele, the level of gene expression was left undetermined. To visualize the Smad2 protein expression, Western blots were run on E10.5 embryo samples. The epitope for Smad2 protein binds to the linker/MH2 region of Smad2, so the presence of Smad2 protein rather than functionality of Smad2 protein is detected. As expected, the samples containing at least one allele of the *3loxP* allele show reduced expression compared to wild-type (WT) samples (Fig. 5). To quantitate the level of *Smad2* mRNA, a real-time polymerase chain reaction (RT-PCR) was run on additional E10.5 embryo samples. RT-PCR measures the amount of mRNA by recording the number of PCR cycles required to replicate enough cDNA to obtain a fluorescence signal from a sample. The RT-PCR primers amplify the region where *neo* cryptic splicing occurs, implying that only

functional mRNA transcripts are detected since primers would be too far separated for RT-PCR amplification when *neo* is cryptically spliced into mRNA. RT-PCR results confirm the decrease in Smad2 expression by Western analysis since the *Smad2*$^{3loxP/-}$ embryos expressed *Smad2* mRNA at about 30-40% the level of WT counterparts (data not shown).

With the hypomorphism of Smad2 confirmed both in genetic and biochemical experiments, the allele was ready to be integrated into various projects investigating Smad2 function. One of these projects was the investigation of Smad2 and Smad3 interactions. As mentioned earlier, most *Smad2*$^{+/-}$*;Smad3*$^{+/-}$ embryos do not survive embryogenesis. In this project the hypomorphic allele allows fine tuning of the *Smad2* levels in contrast to the crude, 50% increment limitations of the *Smad2* null allele [21]. Tweaking the level of Smad2 expression in smaller increments translates into the ability to adjust TGF-β signaling levels in smaller steps so that a more precise level of signaling required for successful embryogenesis can be uncovered.

The new Smad2 hypomorphic allele created four new genotypic combinations of *Smad2* and *Smad3* (*Smad2*$^{3loxP/+}$*;Smad3*$^{+/-}$, *Smad2*$^{3loxP/+}$*;Smad3*$^{-/-}$, *Smad2*$^{3loxP/3loxP}$*;Smad3*$^{+/-}$, and S*mad2*$^{3loxP/3loxP}$*;Smad3*$^{-/-}$), so crosses were arranged to determine the fates of animals carrying these new combinations (Fig. 6). The initial cross between *Smad2*$^{3loxP/3loxP}$ and *Smad3*$^{+/-}$ mice yielded normal pups with the expected genotypes at the expected Mendelian ratios (data not shown). *Smad2*$^{3loxP/+}$*;Smad3*$^{+/-}$ mice were intercrossed, and *Smad2*$^{3loxP/+}$*;Smad3*$^{-/-}$ pups were born with the same phenotype as *Smad3* null mice (data not shown). However, no *Smad2*$^{3loxP/3loxP}$*;Smad3*$^{-/-}$ pups were observed in the F_2 generation, so *Smad2*$^{3loxP/3loxP}$*;Smad3*$^{+/-}$ mice from the F_2 generation were bred *inter se* to increase the expected frequency of *Smad2*$^{3loxP/3loxP}$*;Smad3*$^{-/-}$ pups. At postnatal day twenty-one (the date of weaning), no

Smad2$^{3loxP/3loxP}$*;Smad3*$^{-/-}$ pups were observed, and chi-squared analysis produced a p value of <0.001 (Table 1), suggesting that the particular genotype exhibits embryonic lethality.

Embryos from *Smad2*$^{3loxP/3loxP}$*;Smad3*$^{+/-}$ intercrosses were dissected to confirm embryonic lethality and to investigate the cause of embryonic lethality. Embryos were first dissected between E9.5-E10.5 because embryos with axial patterning defects—the most severe *Smad2*$^{+/-}$*;Smad3*$^{+/-}$ abnormality—survive to E10.5. Expected ratios of embryo genotypes were recovered at E9.5 and E10.5; however, 100% of the *Smad2*$^{3loxP/3loxP}$*;Smad3*$^{-/-}$ embryos were abnormal. Defects included cardiac dysplasia, axial patterning defects, holoprosencephaly (HPE), and delayed development (Table 2). Seventy-five percent of the embryos were affected primarily by some form of cardiac dysplasia, either abnormal heart looping or pericardial effusion (Fig. 7B). Furthermore, all E9.5-E10.5 *Smad2*$^{3loxP/3loxP}$*;Smad3*$^{-/-}$ embryos were smaller than wild-type littermates, and many exhibited craniofacial defects (Fig. 7C). Interestingly, at the same stage of development, about thirty-five percent of *Smad2*$^{3loxP/3loxP}$*;Smad3*$^{+/-}$ embryos were abnormal (Table 2), though none of the defects were as severe as those seen in *Smad2*$^{3loxP/3loxP}$*;Smad3*$^{-/-}$ embryos (Fig. 7B,E). None of the E9.5-E10.5 *Smad2*$^{3loxP/3loxP}$*;Smad3*$^{+/-}$ embryos exhibited axial patterning defects, but the embryos still displayed a variably penetrant phenotype including heart dysplasia, holoprosencephaly, and delayed development (Fig. 7F).

Since hepatic dysplasia was an observed phenotype during studies of *Smad2*$^{+/-}$*;Smad3*$^{+/-}$ embryos, and hepatic dysplasia cannot be discerned until E12.5-E14.5, dissections were performed between E12.5-E14.5 to determine whether any *Smad2*$^{3loxP/3loxP}$*;Smad3*$^{-/-}$ embryos would also succumb to liver abnormalities. At this stage *Smad2*$^{3loxP/3loxP}$*;Smad3*$^{-/-}$ embryos were no longer observed at Mendelian ratios (Table 1), most likely because the embryos with the most severe axial patterning defects and cardiac dysplasia had already begun to resorb. However, the

Smad2$^{3loxP/3loxP}$;*Smad3*$^{-/-}$ embryos that did survive to this stage were all abnormal, as all E12.5-E14.5 *Smad2*$^{3loxP/3loxP}$;*Smad3*$^{-/-}$ embryos suffered from hepatic dysplasia (Fig. 8C,D), while fifty percent also suffered from varying degrees of anterior craniofacial defects including HPE (Fig. 8A, C) and severe anterior truncation (Fig. 8B). Of the forty-nine total *Smad2*$^{3loxP/3loxP}$;*Smad3*$^{+/-}$ embryos observed at this stage (Table 3), twenty-seven percent displayed abnormalities including severe anterior craniofacial truncation, hepatic dysplasia, and HPE. Again, these phenotypes were not mutually exclusive, as three embryos with hepatic dysplasia were also afflicted with varying degrees of HPE.

Discussion

Levels of TGF-β signaling required for embryogenesis

As previously mentioned, the five percent embryonic lethality of *Smad2* heterozygotes suggests that losing fifty percent of functional Smad2 causes the embryos to hover close to the minimum threshold of TGF-β signaling required for viability (Fig. 9). *Smad2* null embryos transgress this threshold, and all embryos exhibit embryonic lethality [11]. *Smad2/3* double heterozygotes also do not produce enough signaling to overcome this threshold, resulting in embryonic lethality, albeit at a later stage of development [21]. My investigations reveal that increasing levels of Smad2 marginally via the *Smad2*$^{3loxP/3loxP}$ allele combination while keeping the level of Smad3 constant in the heterozygous state increases the viability of the embryos to approximately seventy percent. However, replacing the *Smad3*$^{+/-}$ alleles with *Smad3* null alleles decreases viability to 0%. This data suggests that the Smad2 and Smad3 gene dosages appear to determine the severity of the resulting abnormality in a inversely proportional relationship, an observation supported by the *Smad2*$^{3loxP/3loxP}$;*Smad3*$^{+/-}$ embryo defects being less severe than

those of *Smad2*$^{3loxP/3loxP}$*;Smad3*$^{-/-}$ embryos. In addition, the clear importance of Smad2 during development suggests that Smad2 acts as a coarse adjustment of TGF-β signaling levels while Smad3 acts as a fine tuner. This observation was also noted by Dunn *et al*. in their studies of *Smad2/3* interactions at an earlier stage (E6.5-9.5), although they quantitated their approximation of Smad2 contribution versus Smad3 contribution to total TGF-β signaling at each WT *Smad2* allele being worth two WT *Smad3* alleles [27]. These new insights about the amount of Smad2 and Smad3 required for embryogenesis viability are summarized in Table 4.

Origin of variably penetrant phenotypes

Variably penetrant phenotypes were observed with *Smad2*$^{+/-}$*;Smad3*$^{+/-}$, *Smad2*$^{3loxP/3loxP}$*;Smad3*$^{+/-}$, *Smad2*$^{3loxP/3loxP}$*;Smad3*$^{-/-}$, and *Smad2*$^{3loxP/-}$ embryos. *Smad2/3* combinations exhibit four classes of abnormalities including axial patterning defects, cardiac dysplasia, craniofacial defects, and hepatic dysplasia. *Smad2*$^{3loxP/-}$ embryo abnormalities are divided into three classes and, in general, manifest themselves at an earlier stage of development. The three classes are as follows: empty yolk sac, externalized embryo, and axial-patterning defect [12]. The cause of these distinct phenotypes within embryos of the same genotype is intriguing. A potential source is the activity of strain-specific modifier genes. Investigation into the *Smad2/3* double heterozygotes also uncovered variably penetrant phenotypes. However, when the strain background was switched from 129SvEv/NIH Black Swiss to A/J, *Smad2*$^{+/-}$*;Smad3*$^{+/-}$ pups were born alive with no visible abnormalities after one month [21]. Observations of *Smad2*$^{3loxP/3loxP}$*;Smad3*$^{+/-}$ and *Smad2*$^{3loxP/3loxP}$*;Smad3*$^{-/-}$ embryos support the presence of modifiers that adjust the severity of the observed phenotype. For instance, at E9.5-E10.5, all *Smad2*$^{3loxP/3loxP}$*;Smad3*$^{-/-}$ embryos had severe axial defects or heart dysplasia that should have

resulted in resorptions by E13.5, but embryos were observed, though three of the four were from the same litter, suggesting that the embryos were may have expressed a unique combination of modifier genes that mitigated the usual effects of Smad2 and Smad3 depletion.

A continuum of TGF-β signaling via Smad2 and Smad3

The effects of *Smad2* and *Smad3* nullizygosity on embryogenesis have been investigated by many labs, resulting in many alleles that convey a broad spectrum of functional TGF-β signaling. *Smad3* mutations by themselves do not appear to vitally impact embryogenesis since null mice survive to parturition [19, 20]. Smad2, however, plays a fundamental role during embryogenesis, with *Smad2* null embryos exhibiting gastrulation failures at E6.5 and resorbing by E8.5. This was seen in the $Smad2^{mh1}$, $Smad2^{\Delta C}$, $Smad2^{\Delta E9,10}$, and Hamamoto's $Smad2^{-}$ alleles [10-13]. If the Smads transduce enough TGF-β signaling for the embryos to undergo gastrulation, the next threshold arises during anterior/posterior axis specification, as demonstrated by embryos homozygous for severely hypomorphic alleles of *Smad2* such as $Smad2^{Robm1}$, where exon one was replaced with a *neo* cassette; $Smad2^{dex2}$, in which exon two was deleted with a *neo* cassette; and $Smad2^{CD}$, in which exon one was flanked by loxP sites and excised via Cre-mediated recombination [14-16] (Fig. 10). These alleles produce enough Smad2 that TGF-β signaling requirements for gastrulation are met, and mesoderm is formed; however, all embryos homozygous for these alleles were abnormal with the phenotype of an empty yolk sac [14-16]. The empty yolk sac phenotype is also seen when the hypomorphic $Smad2^{m1Mag}$ allele was placed against the $Smad2^{Robm1}$ allele. The $Smad2^{m1Mag}$ allele was created with point mutation techniques to mutate serine-276 to leucine. This serine is not, however, known to participate in any phosphorylation. Regardless, the resulting conformation changes in Smad2 are

severe enough that *Smad2*^{m1Mag} homozygotes are embryonically lethal, albeit enough TGF-β signaling is conveyed for homozygotes to progress further in development and form embryonic structures unlike the previously described alleles. *Smad2*$^{m1Mag/m1Mag}$ embryos display a variably penetrant phenotype that include empty yolk sac, external embryo, and axial/heart defects with anterior truncation [17]. These are the three same phenotypes *Smad2*$^{3loxP/-}$ embryos exhibit, though *Smad2*^{3loxP} homozygotes are viable and fertile [12]. What these two intermediately hypomorphic alleles suggest about TGF-β signaling is that another threshold of signaling occurs during anterior-posterior (A-P) axis specification, since development of embryos similar to *Smad2*^{Robm1} homozygotes arrested before A-P specification [14-16], while marker analysis of external embryos demonstrated A-P specification [21].

Combination of *Smad2* alleles with *Smad3* knockout alleles has yielded intriguing insights into TGF-β signaling mediated synergistically by Smad2 and Smad3 while also uncovering new thresholds. Adding *Smad3* mutations in embryos homozygous for the most severe hypomorphic allele, *Smad2*^{Robm1}, results in a reduction of signaling that limits mesoderm formation [27]. Moving up the threshold ladder, *Smad2*$^{Robm1/+}$*;Smad3*$^{-/-}$ embryos display a range of abnormalities including axial defects, anterior patterning defects [27], and pericardial effusions, all of which have been seen with the least severe class of *Smad2*$^{3loxP/-}$ and *Smad2*$^{m1Mag/m1Mag}$ embryos [12, 17]. In addition, these abnormalities were also seen with the most severe class of *Smad2*$^{3loxP/3loxP}$*;Smad3*$^{-/-}$, *Smad2*$^{3loxP/3loxP}$*;Smad3*$^{+/-}$, and *Smad2*$^{+/-}$*;Smad3*$^{+/-}$ embryos. All of these observations suggest that these four allelic combinations overlap at a TGF-β signaling range that is sufficient for rudimentary anterior patterning, though not enough for embryogenesis to continue past E10.5. In addition, these results support the synergism observation between Smad2 and Smad3 because the addition of *Smad3* null mutations to

Smad2$^{3loxP/3loxP}$ reduces signaling to an extent that abnormalities seen in the least severe, embryonically lethal *Smad2* allele combinations are repeated.

Focusing on embryos older than E7.5, the synergistic cooperation between Smad2 and Smad3 uncovers additional thresholds for TGF-β signaling. After the embryos with severe axial/heart defects have resorbed by E11.5, embryos can still succumb to two abnormalities—craniofacial defects and hepatic dysplasia. Both of these appear dependent on the ligand Nodal. Studies of Nodal, a TGF-β-like ligand that signals via both Smad2 and Smad3, have elucidated its function in heart and anterior patterning [10, 27-30]. Nodal signaling contributes to proper heart patterning [29], so disruption of its signal transducers (Smad2 and Smad3) might lead to the aforementioned heart defects. In addition, embryos heterozygous for *Nodal* mutations have displayed severe anterior truncations [10, 16, 29, 30], which was also seen in a fraction of *Smad2*$^{mh1/+}$ embryos, [10] and in both *Smad2*$^{3loxP/3loxP}$*;Smad3*$^{+/-}$ and *Smad2*$^{3loxP/3loxP}$*;Smad3*$^{-/-}$ embryos. Thus, an anterior patterning threshold exists after axis specification, a threshold at which deficiency results in craniofacial defects.

The final threshold involves meeting the signal requirements for liver development. Interestingly, a fraction of *Nodal* mutants also display hepatic hypoplasia [30]. In addition, Liu *et al*. demonstrated that the *Smad2*$^{+/-}$*;Smad3*$^{+/-}$ liver abnormalities were endodermal in origin [21]. Combining this with increasing evidence that both Smad2 and Smad3 mediate Nodal signals [27], a potential pathway and a possible threshold with its origin in the level of TGF-β signaling arises. This pathway could be masked in mice harboring mutations in either *Smad2* or *Smad3* because enough Smad2 or Smad3 is still present for liver development. The abnormality masking could arise because *Smad2* heterozygote embryos either have enough TGF-β signaling to progress past AP specification/anterior development, or they succumb and resorb.

Considering how Smad2 functions similar to a coarse adjustment, Smad3 mutations might provide the fine adjustment to TGF-β signaling that introduces another threshold level of TGF-β signaling and reveals the synergism between Smad2 and Smad3 for liver development.

These last two thresholds are likely the only ones remaining as far as Smad2/3-influenced thresholds are concerned since *Smad2*$^{3loxP/3loxP}$*;Smad3*$^{+/-}$ embryos were approximately 70% viable, so any abnormalities less severe than hepatic hypoplasia or HPE would be expected to manifest itself with embryos of this genotype. To discern new functions, conditional knockouts will have to be utilized, or *Smad2/3* mutations will have to be compounded with mutations in transcription factors, coactivators, or corepressors. This avenue was investigated when the omnipotent p53 tumor suppressing protein was shown to be capable of binding with Smad2 and Smad3 to regulate transcriptional responses in the *Xenopus* model [31]. To investigate this interaction in the mouse model during embryogenesis, the fates of *p53*$^{-/-}$*;Smad2*$^{+/-}$ pups and *p53*$^{-/-}$*;Smad3*$^{-/-}$ pups was investigated. Pups of both genotypes were found to be viable with no unreported abnormalities over a course of a few months (data not shown), suggesting that, at least for embryogenesis, the interaction between p53 and Smad2 and Smad3 is insignificant.

For future investigations, the suspected endodermal origin of the abnormalities observed in *Smad2*$^{3loxP/3loxP}$*;Smad3*$^{+/-}$ and *Smad2*$^{3loxP/3loxP}$*;Smad3*$^{-/-}$ should be confirmed via marker analysis. In addition, investigation of the hepatic dysplasia observed in the *Nodal* mutants [30] can yield new insights about the mechanism by which Smad2 and Smad3 cause these liver abnormalities.

Materials and Methods

Mice and Genotype analysis

In the above text, *Smad2*$^{-}$ refers to the *Smad2*$^{\Delta C}$ allele unless otherwise mentioned. Mice were maintained on a mixed background of 129Svev and NIH Black Swiss. Genotyping was performed via PCR analysis. DNA samples from toe biopsies or yolk sacs were prepped by standard methods. Detection of *Smad2*^{3loxP} and the *Smad2* wild-type (WT) alleles both use primer 1 (5'-GAG CTG CGC AGA CCT TGT TAC-3') and primer 2 (5'-TGC CTG ACA AAC AGT CCT GG-3'). This primer pair flanks the first loxP site, resulting in an amplification product of ~350 bp for the WT allele and ~450 bp for the *3loxP* allele. Smad2$^{\Delta E9,10}$ was detected using primer 1 and primer 3 (5'-GAA GGG GAT CCC ATC TGA GT-3'), which amplify fragment of ~850 bp [12]. The presence of *Smad2*$^{\Delta C}$ was visualized as ~150 bp fragment using primer 4 (5'-ACT TCG CTA GTT GCT CAT GG-3') and primer 5 (5'-CCA CTT CAT TGC CAT ATG CCC TG-3'). *Smad3* WT allele was detected at ~400 bp using primer 5 and primer 6 (5'-CCC GAA CAG TTG GAT TCA CAC A-3'). The *Smad3* null allele was detected at ~300 bp with primer 5 and primer 7 (5'CCA GAC TGC CTT GGG AAA AGC-3') [20]. WT *p53* alleles were genotyped using primer 7 (5'-ACA GCG TGG TGG TAC CTT AT-3') and primer 8 (5'-TAT ACT CAG AGC CGG CCT-3'), which yielded ~450 bp fragments. Mutant p53 allele was detected using primer 8 and primer 9 (5'-TCC TCG TGC TTT ACG GTA TC-3'), resulting in ~650 bp fragment after PCR analysis.

Embryonic analyses

Dissections were performed in 1X phosphate buffered saline in 0.1% Tween-20 (PBST) and the maternal tissues were dissected away from the embryo and its yolk sac. The yolk sac

was digested to release DNA for genotype analysis, while the embryos were prepped according to the requirements of the subsequent procedure. Pictures were taken with a MTI 3CCD digital camera attached to a Zeiss Stemi SVII Apo dissecting microscope and processed with Scion Series 7 software.

Western Blot

Protein was isolated from embryos that had been dissected according to the above procedure. After cell lysis, Western blots were performed by running the samples on a 10% SDS-Page gel (Biorad), then transferred onto a Hybond™-ECL™ nitrocellulose membrane (Amersham) and probed with anti-Smad2/3 monoclonal IgG antibody (Transduction Labs) that recognizes Smad2 linker region/MH2 domain. After washing, the blot was probed with anti-mouse antibody coupled with alkaline phosphatase (Roche) and visualized using a chemiluminescence kit (Amersham) according to the manufacturer's protocol [21].

Real-time PCR

Embryonic tissues were lysed with by pipetting in Trizol (Invitrogen), and RNA was isolated according to standard procedures. cDNA was replicated from RNA using Superscript III (Invitrogen) according to the manufacturer's protocol. Real-time PCR was prepped using Biorad iQ™ SYBR® Green Supermix for a total of 25 μL per PCR tube. The primers used for the real-time PCR include primer 1 (5'-GAA GGG GAT CCC ATC TGA G-3') and primer 2 (5'-CCC GAA TGT GCA CCA TAA G-3'), which amplify 150 bp fragment of cDNA from the distal end of exon 10 and the proximal portion of exon 11.

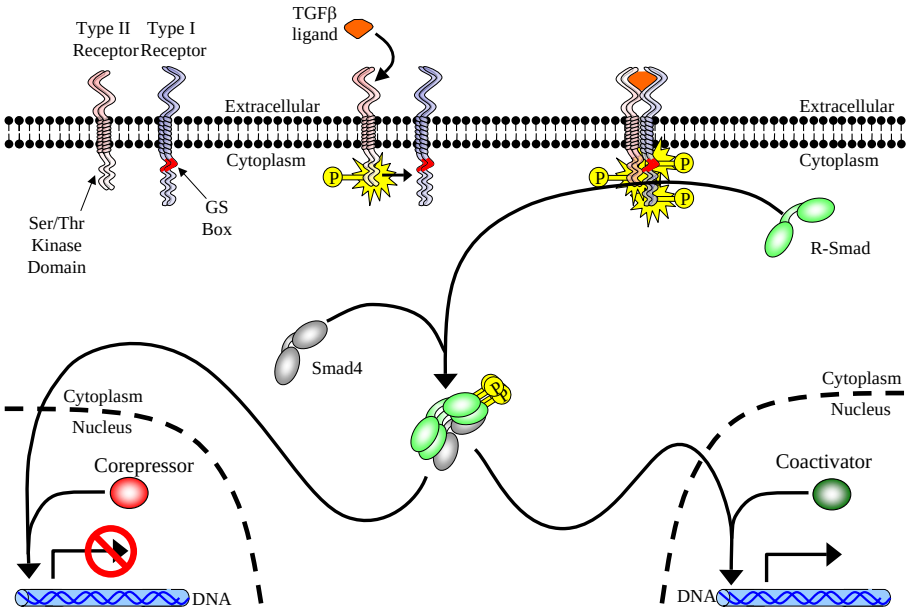

Fig. 1. The TGF-β pathway

Adapted from © 2000 Sinauer Associates, Inc.

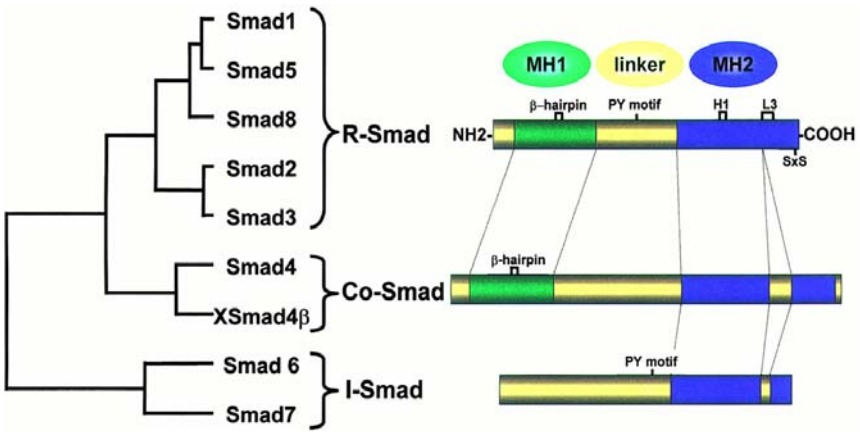

Fig. 2. Homology between R-Smad, Smad4, and I-Smad proteins [3].

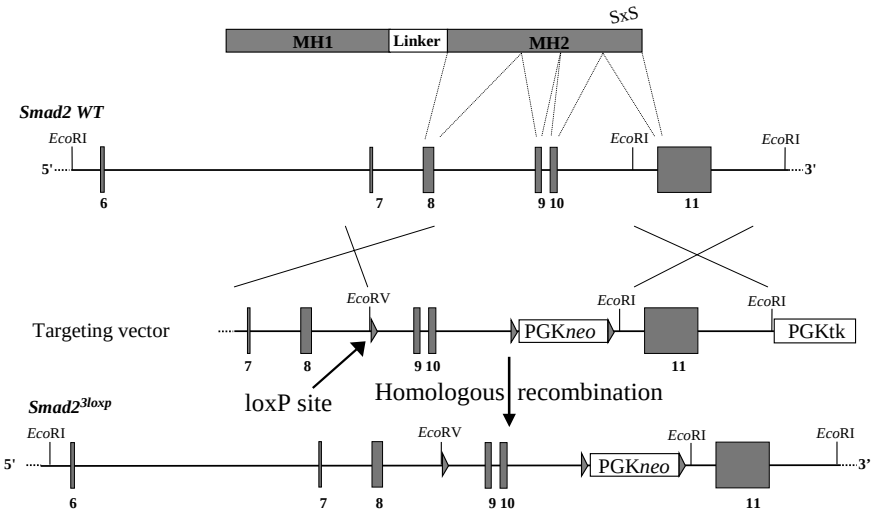

Fig. 3. *Smad2*^{3loxP} allele construction. Modified from [12].

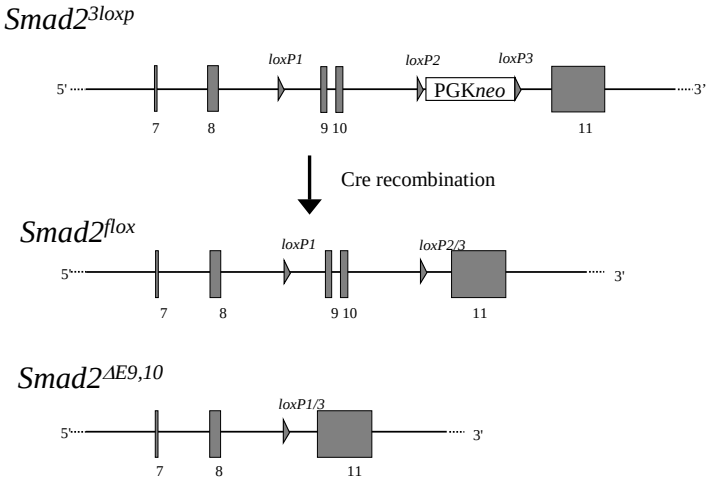

Fig. 4. *Smad2* conditional alleles. Modified from [12]

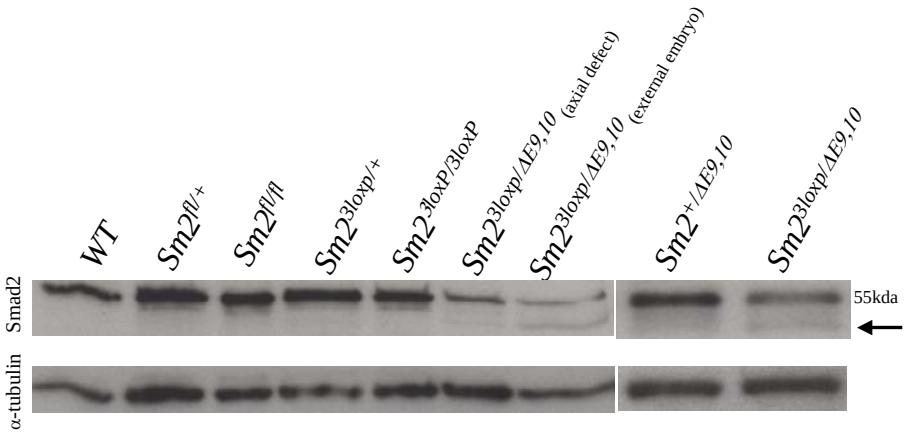

Fig. 5. Western Blot of Smad2 with α-tubulin control; note the decreased Smad2 protein concentration for the *Smad2*$^{3loxP/\Delta E9,10}$ sample compared to the *Smad2*$^{+/\Delta E9,10}$ sample. Arrow points to the suspected truncated protein.

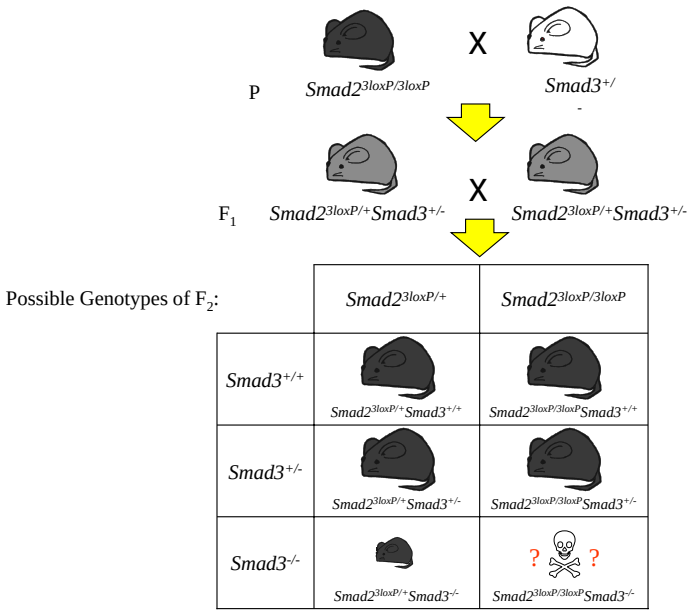

Figure 6. Breeding crosses of the P and F_1 generations. Except for *Smad2*$^{3loxP/3loxP}$*Smad3*$^{-/-}$ pups, all F_2 genotype combinations were observed.

	$Sm2^{3loxp/3loxp}$ $Sm3^{WT}$		$Sm2^{3loxp/3loxp}$ $Sm3^{+/-}$		$Sm2^{3loxp/3loxp}$ $Sm3^{-/-}$			
	Obs	Exp	Obs	Exp	Obs	Exp	Rsp	p
E8.5	5	4.5	11	9	3	4.5	1	0.2
E9.5-E10.5	9 (0)	9	19 (5)	18	8 (8)	9	0	0.92
E13.5	15 (0)	13.25	25 (8)	26.5	4 (4)	13.25	9	0.0034
P21	42 (0)	25	57 (2)	50	0	25	—	<0.001

Table 1. Genotypic analyses of litters resulting from intercrosses of $Smad2^{3loxP/3loxP}Smad3^{+/-}$ mice. Numbers within parentheses denote number of abnormal embryos or mice. Rsp stands for resorption, and P21 is short for postnatal day 21 (the time of weaning). p values are probabilities calculated from χ^2

	$Smad2^{3loxP/3loxP}$	
	$Smad3^{+/-}$	$Smad3^{-/-}$
Axial Abnormality	0	3
Cardiac Dysplasia	4	6
Holoprosencephaly	2	0
Delayed Development	5	0
Resorption	1	0
Total number abnormal	12	8
Sample size	34	8
Percent Abnormal	35%	100%

abnormalities are not mutually exclusive

Table 2. E9.5-E10.5 embryo abnormalities

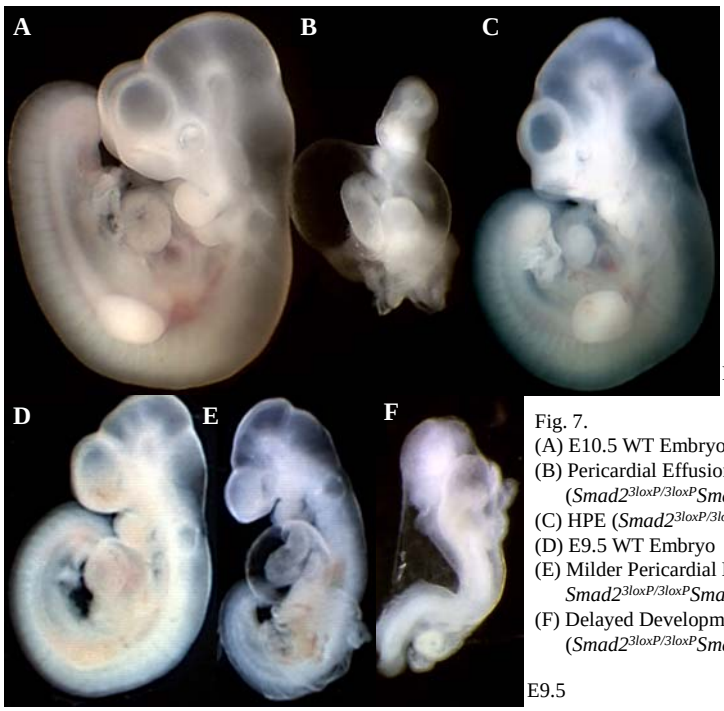

Fig. 7.
(A) E10.5 WT Embryo
(B) Pericardial Effusion (*Smad2*$^{3loxP/3loxP}$*Smad3*$^{-/-}$)
(C) HPE (*Smad2*$^{3loxP/3loxP}$*Smad3*$^{+/-}$)
(D) E9.5 WT Embryo
(E) Milder Pericardial Effusion seen in a *Smad2*$^{3loxP/3loxP}$*Smad3*$^{+/-}$ mutant
(F) Delayed Development (E8.5) (*Smad2*$^{3loxP/3loxP}$*Smad3*$^{+/-}$)

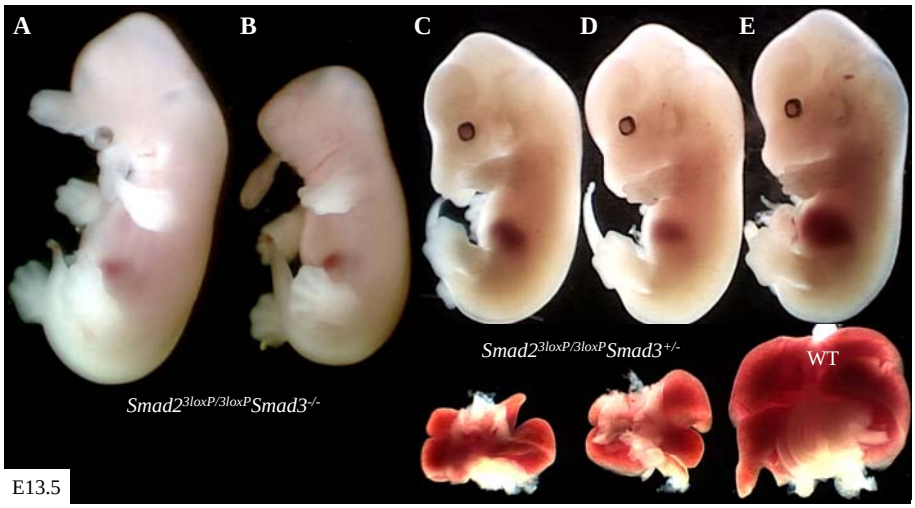

Fig. 8. (A) HPE with proboscis and hypotelorism (B) Severe anterior craniofacial truncation (C) Mild HPE with hepatic dysplasia (D) Hepatic dysplasia only (E) E13.5 WT

	Smad2$^{3loxP/3loxP}$	
	Smad3$^{+/-}$	*Smad3*$^{-/-}$
Hepatic Dysplasia	11	4
Holoprosencephaly	4	2
Anterior Craniofacial Truncation	1	1
Total Number Abnormal	13	4
Sample Size	49	4
Percent Abnormal	27%	100%

phenotypes not mutually exclusive

Table 3. Abnormalities displayed by E12.5-E14.5 embryos.

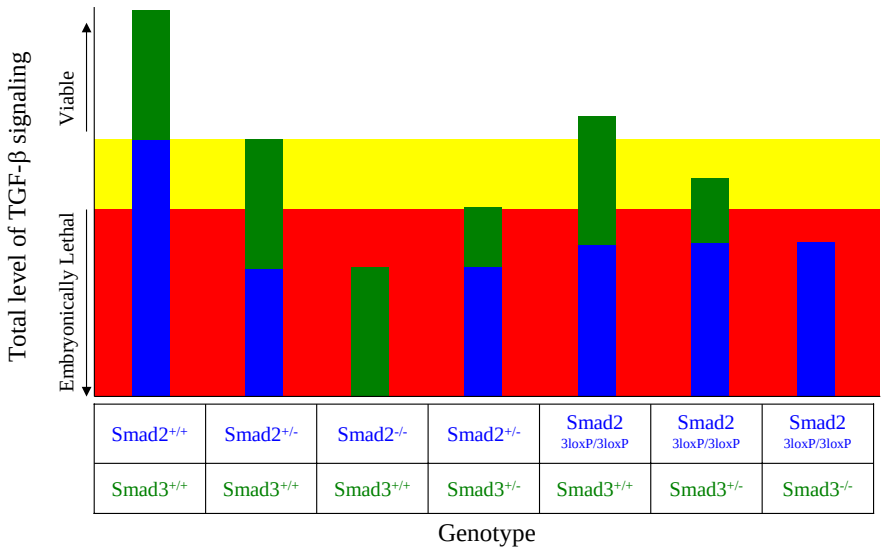

Fig. 9. Levels of Smad2 and Smad3 required for viability; bars with total level of TGF-β signaling in the red zone are embryonically lethal, bars in the yellow zone exhibit a mixture of lethality and viability, and bars completely above the yellow zone are completely viable. The approximate ratio of total Smad2 : total Smad3 contributions to total TGF-β signaling borrowed from [27].

Decreasing *Smad2* Transcription

Decreasing *Smad3* Transcription

	Smad2 +/+	*Smad2* +/*3loxp*	*Smad2* *3loxp*/*3loxp*	*Smad2* +/-	*Smad2* *3loxp*/-	*Smad2* -/-
Smad3 +/+	WT	WT	WT	95% viable	Lethal by E10.5	Lethal by E6.5
Smad3 +/-	WT	WT	~70% viable	Lethal by E16.5		
Smad3 -/-	Viable (Sterile)	Viable (Sterile)	Lethal by E16.5			

Table 4. Levels of *Smad2* and *Smad3* required for viability

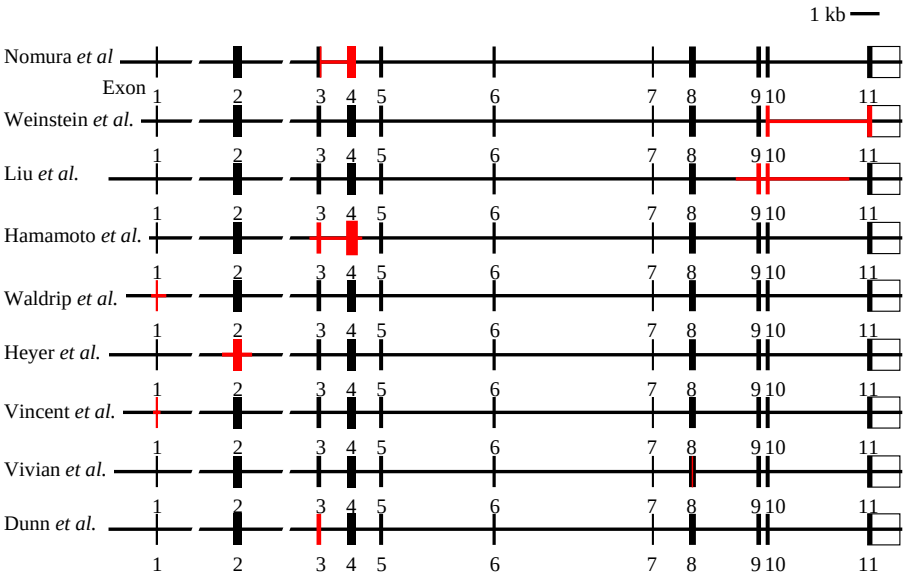

Fig. 10. In red are the regions of the *Smad2* locus that have been targeted for deletion. Adapted and expanded from [18]

References

1. Blobe, G.C., Schiemann, W.P., Lodish, H.F., *Role of transforming growth factor β in human disease.* New England Journal of Medicine, 2000. **342**: p. 1350-1358.
2. ten Dijke, P., Hill, C.S., *New insights into TGF-β–Smad signalling.* TRENDS in Biochemical Sciences, 2004. **29**(5): p. 265-273.
3. Itoh, S., Itoh, F., Goumans, M.J., ten Dijke, P., *Signaling of transforming growth factor-beta family members through Smad proteins.* Eur J Biochem., 2000. **267**(24): p. 6954-6967.
4. Massague, J., *TGFbeta signaling: receptors, transducers, and Mad proteins.* Cell, 1996. **85**(7): p. 947-950.
5. Hahn, S.A., Schutte, M., Hoque, A.T., Moskaluk, C.A., da Costa, L.T., Rozenblum, E., Weinstein, C.L., Fischer, A., Yeo, C.J., Hruban, R.H., Kern, S.E., *DPC4, a candidate tumor suppressor gene at human chromosome 18q21.1.* Science, 1996. **271**(5247): p. 350-353.
6. Heldin, C.H., Miyazono, K., ten Dijke, P., *TGF-beta signalling from cell membrane to nucleus through SMAD proteins.* Nature, 1997. **390**(6659): p. 465-471.
7. Tian, F., DaCosta Byfield, S., Parks, W.T., Yoo, S., Felici, A., Tang, B., Piek, E., Wakefield, L.M., Roberts, A.B., *Reduction in Smad2/3 signaling enhances tumorigenesis but suppresses metastasis of breast cancer cell lines.* Cancer Res., 2003. **63**(23): p. 8284-8292.
8. Han, S.U., Kim, H.T., Seong, D.H., Kim, Y.S., Park, Y.S., Bang, Y.J., Yang, H.K., Kim, S.J., *Loss of the Smad3 expression increases susceptibility to tumorigenicity in human gastric cancer.* Oncogene, 2004. **23**(7): p. 1333-1341.
9. Zhu, Y., Richardson, J.A., Parada, L.F., Graff, J.M., *Smad3 mutant mice develop metastatic colorectal cancer.* Cell, 1998. **94**(6): p. 703-714.
10. Nomura, M., Li, E., *Smad2 role in mesoderm formation, left-right patterning and craniofacial development.* Nature, 1998. **393**(6687): p. 786-790.
11. Weinstein, M., Yang, X., Li, C., Xu, X., Gotay, J., Deng, C.X., *Failure of egg cylinder elongation and mesoderm induction in mouse embryos lacking the tumor suppressor smad2.* Proc Natl Acad Sci U S A., 1998. **95**(16): p. 9378-83.
12. Liu, Y., Festing, M.H., Hester, M., Thompson, J.C., Weinstein, M., *Generation of novel conditional and hypomorphic alleles of the Smad2 gene.* Genesis, 2004. **40**(2): p. 118-123.
13. Hamamoto, T., Beppu, H., Okada, H., Kawabata, M., Kitamura, T., Miyazono, K., Kato, M., *Compound disruption of smad2 accelerates malignant progression of intestinal tumors in apc knockout mice.* Cancer Res., 2002. **62**(20): p. 5955-5961.
14. Waldrip, W.R., Bikoff, E.K., Hoodless, P.A., Wrana, J.L., Robertson, E.J., *Smad2 signaling in extraembryonic tissues determines anterior-posterior polarity of the early mouse embryo.* Cell, 1998. **92**(6): p. 797-808.
15. Heyer, J., Escalante-Alcalde, D., Lia, M., Boettinger, E., Edelmann, W., Stewart, C.L., Kucherlapati, R., *Postgastrulation Smad2-deficient embryos show defects in embryo turning and anterior morphogenesis.* Proc Natl Acad Sci U S A., 1999. **96**(22): p. 12595-12600.

16. Vincent, S.D., Dunn, N.R., Hayashi, S., Norris, D.P., Robertson, E.J., *Cell fate decisions within the mouse organizer are governed by graded Nodal signals.* Genes Dev., 2003. **17**(13): p. 1646-1662.
17. Vivian, J.L., Chen, Y., Yee, D., Schneider, E., Magnuson, T., *An allelic series of mutations in Smad2 and Smad4 identified in a genotype-based screen of N-ethyl-N-nitrosourea-mutagenized mouse embryonic stem cells.* Proc Natl Acad Sci U S A., 2002. **99**(24): p. 15542-15547.
18. Dunn, N.R., Koonce, C.H., Anderson, D.C., Islam, A., Bikoff, E.K., Robertson, E.J., *Mice exclusively expressing the short isoform of Smad2 develop normally and are viable and fertile.* Genes Dev., 2005. **19**(1): p. 152-163.
19. Datto, M.B., Frederick, J.P., Pan, L., Borton, A.J., Zhuang, Y., Wang, X.F., *Targeted disruption of Smad3 reveals an essential role in transforming growth factor beta-mediated signal transduction.* Mol Cell Biol., 1999. **19**(4): p. 2495-2504.
20. Yang, X., Letterio, J.J., Lechleider, R.J., Chen, L., Hayman, R., Gu, H., Roberts, A.B., Deng, C., *Targeted disruption of SMAD3 results in impaired mucosal immunity and diminished T cell responsiveness to TGF-beta.* EMBO J., 1999. **18**(5): p. 1280-1291.
21. Liu, Y., Festing, M., Thompson, J.C., Hester, M., Rankin, S., El-Hodiri, H.M., Zorn, A.M., Weinstein, M., *Smad2 and Smad3 coordinately regulate craniofacial and endodermal development.* Dev Biol., 2004. **270**(2): p. 411-426.
22. Weinstein, M., Monga, S.P., Liu, Y, Brodie, S.G., Tang, Y., Li, C., Mishra, L., Deng, C.X., *Smad proteins and hepatocyte growth factor control parallel regulatory pathways that converge on beta1-integrin to promote normal liver development.* Mol Cell Biol., 2001. **21**(15): p. 5122-5131.
23. Sauer, B., *Inducible gene targeting in mice using the Cre/lox system.* 1998, 1998. **14**(4): p. 381-392.
24. Bockamp, E., Maringer, M., Spangenberg, C., Fees, S., Fraser, S., Eshkind, L., Oesch, F., Zabel, B., *Of mice and models: improved animal models for biomedical research.* Physiol Genomics, 2002. **11**(3): p. 115-132.
25. Meyers, E.N., Lewandoski, M., Martin, G.R., *An Fgf8 mutant allelic series generated by Cre- and Flp-mediated recombination.* Nat Genet., 1998. **18**(2): p. 136-141.
26. Hester, M., Thompson, J.C., Mills, J., Liu, Y., El-Hodiri, H.M., Weinstein, M., *Smad1 and Smad8 function similarly in mammalian central nervous system development.* Mol Cell Biol., 2005. **25**(11): p. 4683-4692.
27. Dunn, N.R., Vincent, S.D., Oxburgh, L., Robertson, E.J., Bikoff, E.K., *Combinatorial activities of Smad2 and Smad3 regulate mesoderm formation and patterning in the mouse embryo.* Development, 2004. **131**(8): p. 1717-1728.
28. Brennan, J., Norris, D.P., Robertson, E.J., *Nodal activity in the node governs left-right asymmetry.* Genes Dev., 2002. **16**(18): p. 2339-2344.
29. Norris, D.P., Brennan, J., Bikoff, E.K., Robertson, E.J., *The Foxh1-dependent autoregulatory enhancer controls the level of Nodal signals in the mouse embryo.* Development, 2002. **129**(14): p. 3455-3468.
30. Lowe, L.A., Yamada, S., Kuehn, M.R., *Genetic dissection of nodal function in patterning the mouse embryo.* Development, 2001. **128**(10): p. 1831-1843.
31. Cordenonsi, M., Dupont, S., Maretto, S., Insinga, A., Imbriano, C., Piccolo, S., *Links between tumor suppressors: p53 is required for TGF-beta gene responses by cooperating with Smads.* Cell, 2003. **113**(3): p. 301-314.